Charles L. Asbury[1]
Alan H. Diercks[2]
Ger van den Engh[2]

[1]Biological Sciences,
Stanford University,
Stanford, CA, USA
[2]Institute for Systems Biology,
Seattle, WA, USA

Trapping of DNA by dielectrophoresis

Under suitable conditions, a DNA molecule in solution will develop a strong electric dipole moment. This induced dipole allows the molecule to be manipulated with field gradients, in a phenomenon known as dielectrophoresis (DEP). Pure dielectrophoretic motion of DNA requires alternate current (AC) electric fields to suppress the electrophoretic effect of the molecules net charge. In this paper, we present two methods for measuring the efficiency of DEP for trapping DNA molecules as well as a set of quantitative measurements of the effects of strand length, buffer composition, and frequency of the applied electric field. A simple configuration of electrodes in combination with a microfluidic flow chamber is shown to increase the concentration of DNA in solution by at least 60-fold. These results should prove useful in designing practical microfluidic devices employing this phenomenon either for separation or concentration of DNA.

Keywords: Dielectrophoresis / DNA separation / Microfluidics EL 5079

1 Introduction

The response of DNA strands in solution to a uniform electric field, known as electrophoresis, is well known and is fundamental to many common separation techniques. Less well studied is the effect, often referred to as dielectrophoresis (DEP) [1], that induced dipole forces have on the behavior and DNA. Earlier work [2–4] has demonstrated that regions of modest electric field and high field gradient can induce a dipole moment in DNA and cause it to aggregate. The ability to manipulate DNA using its induced dipole moment offers exciting possibilities for the development novel separation schemes and controlled movement of small quantities of molecules, yet few studies of DEP applied to DNA have been made, and little is known about the important parameters which govern the strength of the effect. A sound physical understanding of DEP is critical to development of practical applications and particularly important for microelectrofluidic devices which often subject DNA to high field gradients due to the small size of their electrodes [5].

Like other charged particles in solution, DNA possesses a counterion cloud which is responsible for its large polarizability at low frequency ($\sim$ 10 kHz). This "anomalous" polarizability, so-called because it is not explained by Maxwell-Wagner theory, is well-known and readily seen in bulk dielectric measurements of DNA solutions [6–14]. Although these bulk dielectric measurements provide quantitative information about how the strength of the induced dipole is expected to scale with molecule size, buffer compositon, and applied frequency, the applicability of these studies to DEP of individual molecules is not clear. Whereas the bulk measurements use weak, uniform electric fields, DNA experiencing DEP in microdevices is subject to high fields and strong, localized field-gradients which vary on scales comparable to the strand length. Furthermore, agreement between various bulk studies is poor, and interpreting the data in terms of simple theory is complicated by the length and flexibility of the DNA chain.

In this paper we describe two methods for measuring the strength and capacity of dielectrophoretic DNA traps. Trapping efficiency was measured as a variety of parameters were varied, including the strand length, the strength and frequency of the applied field, and the ionic concentration of the solution. The first method uses a CCD camera and fluorescence microscope to take a sequence of digital images as the trapping voltage is turned on and then off again. The second method uses a microfluidic channel placed over the trapping electrodes and a photomultiplier to measure the fluorescence from small quantities of DNA trapped and subsequently released upstream of the measurement point. The results from both methods provide information about the mechanism(s) of polarization of DNA and guide efforts to apply DNA trapping in practical devices.

2 Materials and methods

2.1 Method 1: quantitation from digital images

Samples contained λ-phage DNA (48.5 kb) of smaller DNA fragments (adenovirus, 35.9 kb, and pBR322, 4.4 kb; Gibco BRL, Gaithersburg, MD, USA), diluted to the same final weight fraction (180 ng/mL = 270 nM bp) in

Correspondence: Dr. Alan H. Diercks, Institute for Systems Biology, 4225 Roosevelt Way NE, Seattle, WA 98102, USA
E-mail: diercks@systemsbiology.org
Fax: +206-732-1253

Abbreviations: DEP, dielectrophoresis; **PDMS**, polydimethylsiloxane

© 2002 WILEY-VCH Verlag GmbH & Co. KGaA, Weinheim 0173-0835/02/1608–2658 $17.50+.50/0

deionized water + YOYO dye (Molecular Probes, Eugene, OR, USA). Samples in Tris-buffer at varying concentrations were made by adding Tris-HCl (pH 8.5) to stock λ-phage DNA prior to dilution. The final dye concentration in all experiments was 200 nM. The method of quantitation from digital images has been described previously [2]. Briefly, a CCD camera attached to an epifluorescence microscope recorded the motion of fluorescence-labeled DNA molecules as they were trapped and then released. Oscillating electric fields with strong gradients were generated using a repeating pattern of thin gold-film strips deposited onto a quartz substrate using standard microlithographic techniqes. Typically, 100 strips of metal film were deposited onto the central 10 × 10 mm area of an 18 × 18 × 1 mm quartz chip. Metal films consisted of a 2 nm adhesion layer of chrome followed by a 4-nm layer of gold. The strips were 70 μm wide, separated by 30 μm gaps. Five microliters of a liquid sample containing DNA was sandwiched between the microelectrodes and a glass cover-slip, and sealed with molten agarose (see Fig. 1 of [2]. Although no direct electrical connection was made to the electrodes, electric fields applied to the fluid were strongly concentrated near the edges due to their extreme thinnes (~ 6 nm) and high conductivity relative to the fluid.

The CCD camera was programmed to take a sequence of 250 ms exposures of the device at a rate of one per second with the first exposure taken before the application of voltage. The oscillating voltage (30 Hz, 200 V_{p-p} applied across the slide) was switched on just prior to the second exposure and switched of again after 30 s. Profiles of fluorescence across the gold-film strips were obtained by integrating the images parallel to the strips. Each profile was normalized to account for the slow decrease of fluorescence over the course of each experiment, as well as variations in illumination intensity between experiments. A series of images showing DNA trapping over electrode edges is displayed in Fig. 1.

2.2 Method 2: point-measurements of trapping in a microfluidic channel

This method was devised to make measurements of DNA trapping with better repeatability than was achieved with the CCD-based method. The improvements included (i) a buffered salt solution in which the DNA was suspended, (ii) sealed microdevices for control or suppression of solvent flow, and (iii) a custom-built confocal microscope for fluorescence quantitation.

2.2.1 Preparation of DNA samples

Stock solution (125 μg/mL) of four different molecular weights of DNA (T2 phage, 164 kb; λ-phage, 48.5 kb; adenovirus, 35.9 kb; pBR322, 4.4 kb) were diluted to 5 μg/mL in a Tris-buffered saline solution (12.5 mM Tris, 1.25 mM EDTA, and 12.5 mM NaCl, pH 8.5). YOYO-1 dye was diluted to 10 μM in deionized water. Stained samples

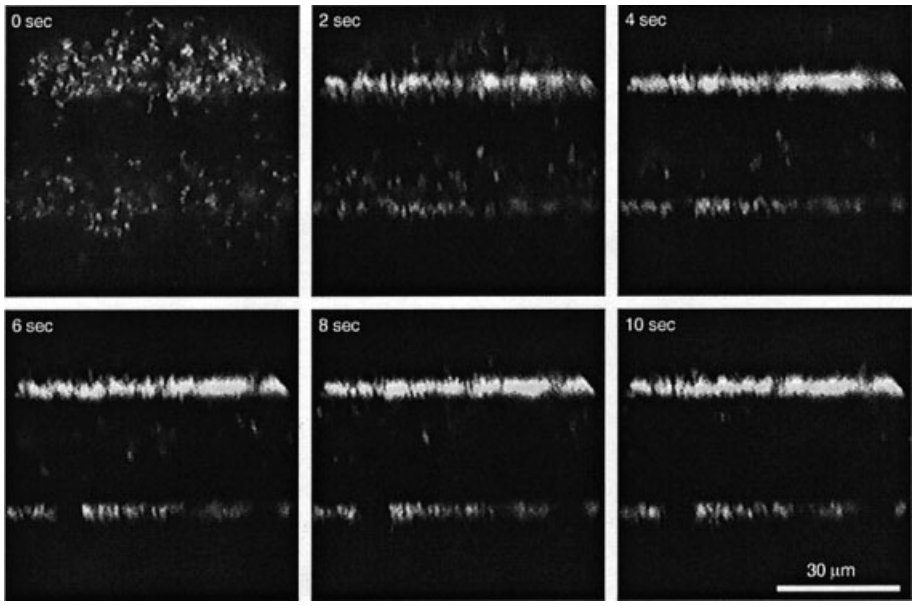

Figure 1. Time series showing DNA trapping. YOYO-stained λ-phage DNA molecules were trapped in a floating-electrode device sealed with molten agarose, as described in Method 1 of this paper and in [2] (see Fig. 1 of [2]). A 30 Hz, 200 V_{p-p} signal was applied to the platinum wires just after the first image was captured (upper left, 0 s). Molecules that were initially within ~ 10 μm of an electrode edge when the field was applied were trapped immediately, while molecules further away accumulated over time. A slow, unintended sample flow or a slight direct current (CD) bias in the applied voltage may have caused more molecules to be trapped at the edge of the upper electrode than at the lower electrode (see Section 3.1).

were made immediately prior to use by mixing these two solutions with deionized water in the proportion 47:2:1 (dH_2O:DNA:YOYO), resulting in final concentrations of 200 ng/mL DNA (300 nM bp), 200 nM YOYO, 0.5 mM Tris, 0.05 mM EDTA, and 0.5 mM NaCl.

2.2.2 Microfabrication of sealed chambers with internal electrodes

Interdigitated electrodes were patterned onto glass cover-slips, using standard microlithographic techniques. A 2 nm adhesion layer of chrome was followed by an 18 nm layer of gold. The interdigitations were 170 μm wide, separated by 30 μm gaps on either side. Channels were cast into polydimethylsiloxane (PDMS, "Sylgard"; Dow Corning, Midland, MI, USA) using a negative mold consisting of a silicon wafer with a thick (15 μm) photoresist patterned onto it. The cured PDMS rubber was optically clear and adhered to clean glass surfaces by electrostatic attraction. Placing the PDMS onto the patterned cover-slips created sealed chambers (15 μm × 100 μm × 15 mm) with the electrodes inside (Fig. 2). Inlet and outlet ports were created by punching small holes through the PDMS. Measurements could be made with a high magnification oil immersion lens from below (through the cover-slip) or with a long working distance lens from above (through the PDMS). The devices could be peeled apart, cleaned, and reused indefinitely. Devices were filled by pipetting 10 μL of DNA solution into the inlet port and applying suction to the outlet port. Gentle flow was then induced by creating a hydrostatic pressure difference between the ports. For example, filling the inlet port of the device in Fig. 2 to a level 1–2 mm higher than the outlet resulted in a flow rate of ~1 nL/min. Pipette tips were inserted into the ports to shield the free surface of the liquid from air currents that disrupted the steady flow. The interdigitated electrodes used in this method required much lower voltage to achieve DNA trapping than the floating electrodes used in Method 1 (typically 0.5–4 V_{p-p}, rather than 200 V or more). Making directed connections to the electrodes also avoided uncertainty in the voltage achieved. To make the connections, wires were glued with silver epoxy to large gold-film connection-pads that extended out from under the PDMS channel. Trapping voltages were supplied by a commercial function generator (DS345; Stanford Research Systems, Palo Alto, CA, USA). Whenever the trapping voltage was switched off, the gold-film electrodes were immediately shorted together, preventing capacitive discharge currents from flowing through the DNA solution and ensuring that the behavior of the molecules did not depend on the exact phase of the switching relative to the trapping signal.

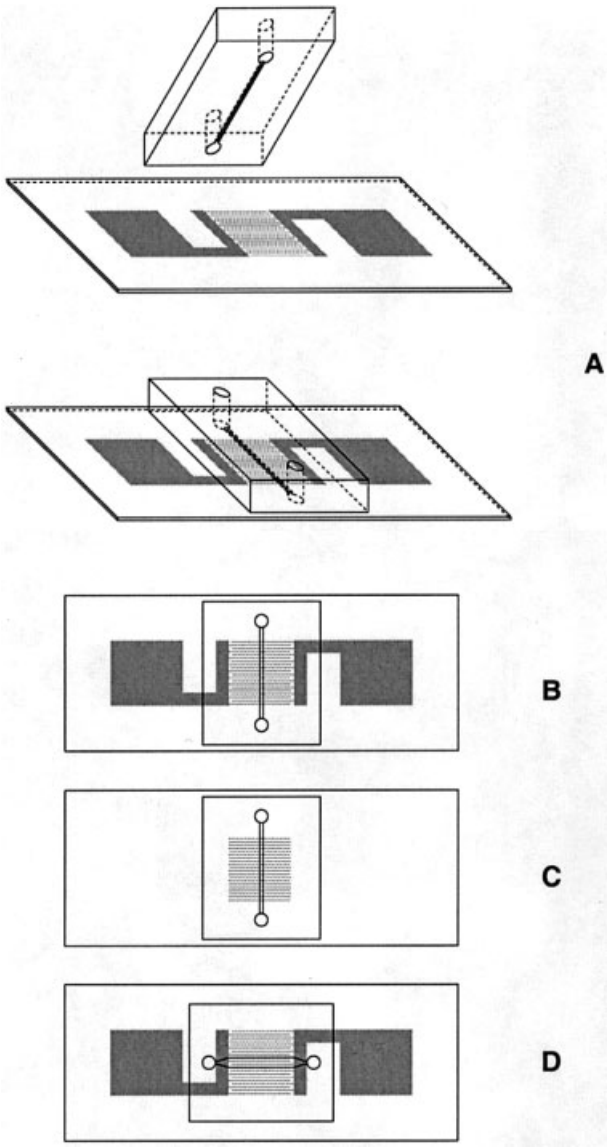

Figure 2. (A) A block of silicone elastomer (PDMS) with a channel (100 μm × 15 μm, *w* × *h*) cast into it adheres to a glass cover-slip with gold-film electrodes, creating a sealed device. Holes punched through the silicone form inlet and outlet ports, which allow the chambers to be filled by suction. (B)–(D) Various combinations of channel and electrode geometry can be combined for different applications.

2.2.3 Design of the confocal measurement microscope

A custom-built microscope was used to simultaneously observe and quantitate fluorescence from stained DNA molecules. The instrument was similar to a modern inverted microscope with the addition of a pinhole-mirror at the image plane of the tube lens. The defocused beam

of an argon-ion laser (2213-75SLYW; Cyonics, San Jose, CA, UDA) was used as the illumination source. Real-time observation of the DNA molecules was possible because an image of the pinhole-mirror, and of the magnified molecules parfocal with it, was projected onto an intensified camera (VE1000-SIT; Dage MIT, Michigan City, IN, USA). Light passing through the pinhole was simultaneously measured by a photomultiplier tube (H5783; Hamamatsu, Japan). The pinhole acted as a spatial filter, allowing only light from the measurement area to reach the photomultiplier. The size of the illuminated area was controlled by a diaphragm aperture, and could be limited during data collection to the area immediately around the pinhole. Thus, photo-induced bleaching and strand-breakage of molecules prior to measurement was completely avoided. Output of the photomultiplier was amplified and low-pass filtered (SR570; Standard Research Systems, Palo Alto, CA, USA) prior to digitization at 10 samples/s and storage on a personal computer. Intensity values were normalized so that the highest value from a set of measurements was unity. Background subtraction was not performed, so measurements contained small offsets that depended on the photomulitplier gain setting.

2.3 Measurement procedure

The device in Fig. 2 was filled with a DNA solution, and a gentle flow of $\sim$ 1 nL/min was generated in the channel by hydrostatic pressure. Movement of the molecules was observed by peering between two adjacent gold-film electrodes through the cover-slip. The cross-section of the channel was 100 μm $\times$ 15 μm, resulting in an average speed of 10 μm/s for the DNA. Molecules near the walls of the channel moved more slowly than average, because of the viscous drag exerted on the fluid by the chamber walls. Fluorescence from trapped molecules was quantitated by placing the confocal measurement point downstream of the electrode nearest the inlet port. Because only the first electrode was upstream of the measurement point, a single peak representing the quantity of DNA trapped at one electrod was detected for each measurement cycle. When a trapping voltage (typically between 0.5 and 4 V_{p-p}, and 5–2000 Hz) was applied, molecules began to accumulate over the edge of the upstream electrode. Accumulation continued as long as voltage was applied because upstream molecules were continuously being transported by the flow to the vicinity of the trap. Switching the trapping voltage off released an accumulation of molecules which flowed past the measurement point, causing a large spike in the photomultiplier output. The magnitude of this spike was taken as a measure of the trapping efficiency. Voltage, frequency, or duration of the applied signal could be altered between consecutive measurements of the same sample, allowing repeated comparisons of trapping efficiency as these parameters were varied.

3 Results

3.1 Method 1

The fluorescence profiles shown in Fig. 3 illustrate the typical time behavior of DNA trapping using Method 1. As soon as the trapping field was switched on, narrow peaks of fluorescence ($\sim$ 5 μm in width) grew rapidly in the profiles where DNA molecules became concentrated over the edges of the gold-film electrodes. The field was switched off again after 30 s and the peaks broadened and shortened as the DNA molecules dispersed.

Despite considerable variation between experiments, useful information was obtained by making repeated measurements and comparing the peak heights achieved

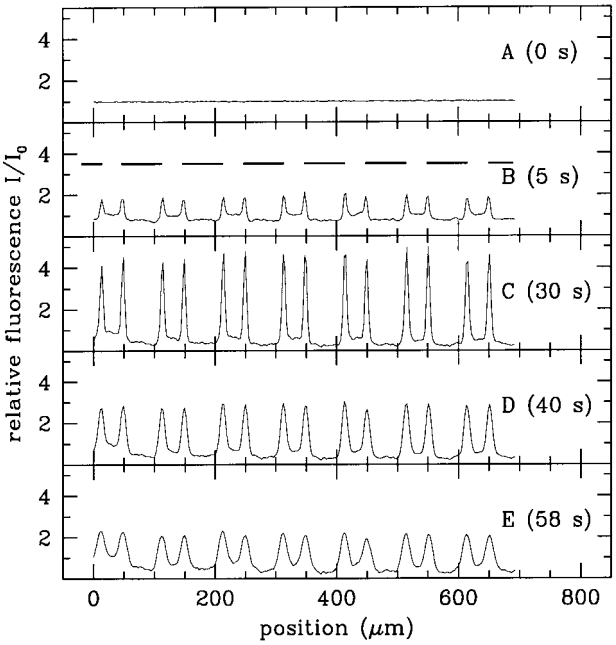

Figure 3. CCD camera measurements of DNA trapping over electrode edges. Fluorescence profiles were obtained from CCD exposures by integrating the digital images parallel to the edges of the gold-film strips. The positions of the electrodes are indicated in (B). Selected profiles from a sequence taken as the trapping field was switched on and then off again show the buildup and dispersal of trapped DNA molecules. (A)–(C) Immediately after the field was applied, narrow peaks of fluorescence grew rapidly where DNA became concentrated over the electrode edges. (D), (E) After 30 s, the field was switched off, and the peaks broadened and shortened as the molecules dispersed.

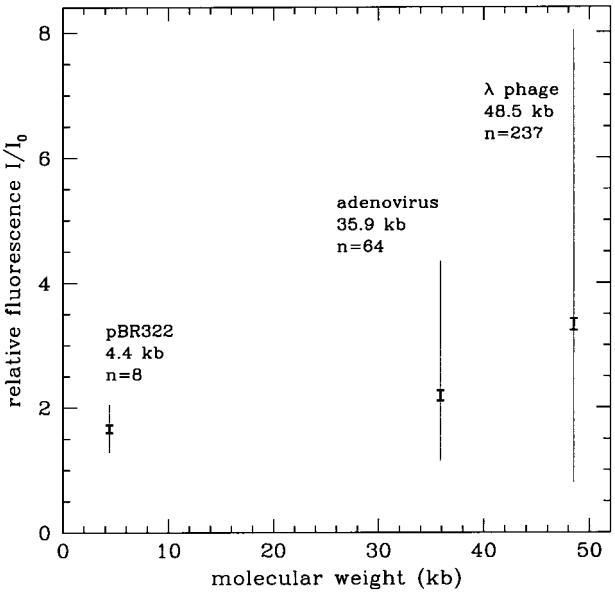

Figure 4. Dependence of trapping efficiency on DNA molecular weight. Fluorescence peak height distributions after 30 s of applied voltage (30 Hz, 200 V_{p-p}) indicate a slight tendency for larger molecules to be more easily trapped. "n" denotes the number of peaks measured for each condition. The thick bars extend one standard error above and below the mean while the thin bars encompass all the data. A K-S test verifies that the λ-phage and adenovirus distributions are significantly different at the $P \sim 10^{-8}$ level. $P = 7 \times 10^{-3}$ between the adenovirus and pBR322 distributions.

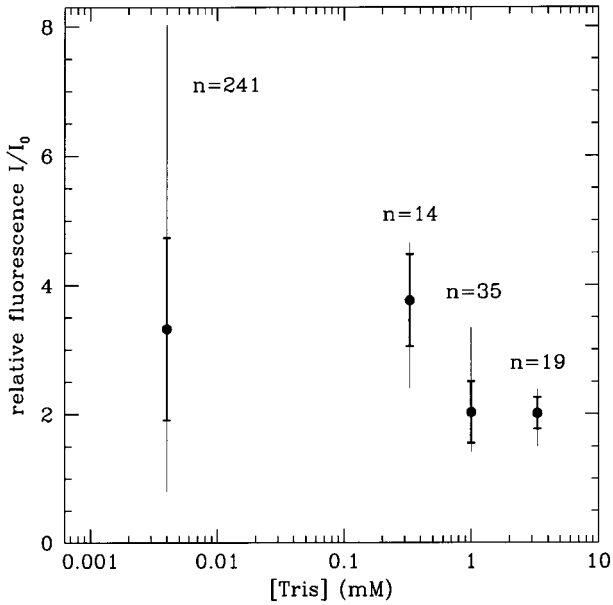

Figure 5. Effect of added Tris-HCl on trapping efficiency. Peak height distributions after 30 s of applied voltage (30 Hz, 200 V_{p-p}) show evidence for a significant decrease in trapping efficiency above Tris concentrations of 1 mM. "n" denotes the number of peaks measured for each condition. Samples with the lowest concentration of Tris (0.004 mM) were dilutions of the Gibco stock solution into deionized water. No measurable increase in fluorescence over the electrode edges occurred for Tris concentrations greater than 3.3 mM (data not shown).

after 30 s of applied voltage. The heights of ~ 300 fluorescence peaks measured in 23 separate experiments with different size DNA molecules are compared in Fig. 4. The distributions are broad, but they indicate a statistically significant trend for larger molecules to produce higher peaks. The effect of adding Tris-buffer to the samples was also investigated in ten experiments. Peak heights obtained with different concentrations of Tris-HCl are compared in Fig. 5. The addition of more than ~ 1 mM buffer tended to decrease the measured peak heights. No measurable peaks were obtained when the concentration of Tris-HCl was 10 mM or higher. At the lowest salt concentrations used in these experiments (0.1 mM) DNA denaturation becomes a concern as the melting temperature can approach room temperature [15]. Denaturation is known to weaken the polarizability of DNA [7, 16] and is potentially responsible for the leveling off of the trapping efficiency shown in Fig. 5. However, we observed no direct evidence for denaturation such as decreased fluorescence from the intercalating YOYO dye.

The method of assembling the trapping devices with agarose (see [2], Fig. 1) was crude, and it was difficult to completely suppress the flow of liquid between the coverslips. Consequently, a slow, directed transport of the molecules often occurred even before the application of electrical forces. This bulk flow continued during application of the trapping field and subsequent release of the molecules. When flow perpendicular to the traps occurred, it increased the rate of trapping by sweeping molecules into the traps and caused an asymmetry in the trapping over opposite edges. Fewer molecules were trapped over the electrode edges facing "into" the flow, although the reasons for this asymmetry are unclear [2]. We believe that uncontrolled fluid movement in the device and slight differences in the conductivity of the medium are largely responsible for the significant variations between experiments using this method. An improved flow control system which kept the fluid at rest as well as allowed flow at a well controlled rate, would permit measurement of trapping efficiency as a function of low velocity.

At low frequencies (< 30 Hz), trapped molecules were observed to execute oscillatory motion over the electrode edges with an approximate amplitude of 5 μm, presumably due to electrophoresis. This interpretation is supported by experiments at much lower frequencies

(~ 3 Hz), where the amplitude was considerably larger. The fact that the molecules remained trapped over the electrode edges in our experiments, rather than being alternately pushed and pulled away in response to the changing polarity of the driving field, suggests that in these experiments the dielectrophoretic effect dominated over electrophoretic motion.

3.2 Method 2

Figure 6 shows the fluorescence intensity *versus* elapsed time during a typical experiment applying Method 2 to T2 phage DNA (164 kb), in which the frequency of the applied field was varied for each measurement. At each frequency, 3 V_{p-p} was applied for 60 s, followed by a 30 s interval with no voltage. A slight decrease in fluorescence is evident during voltage application, indicating that a significant fraction of molecules flowing past the upstream electrode were being trapped. Bright spikes occurred immediately after the voltage was switched off as the previously trapped molecules flowed past the detector. The height of the peak was used as a measure of the quantity of trapped DNA. The area of each peak could also have been used, but peak height was simpler to obtain and the peaks always had similar shape, making the results independent of this choice.

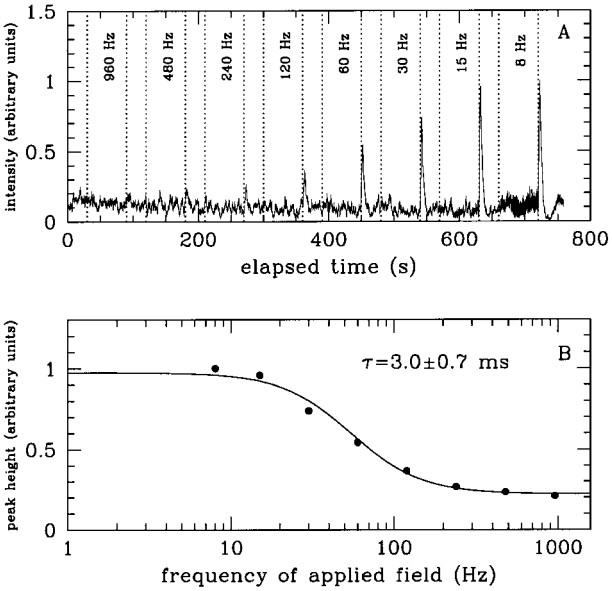

Figure 6. Dependence of trapping efficiency on frequency. (A) Fluorescent intensity *versus* elapsed time during an experiment in which the frequency of the trapping field was varied. Bright spikes occurred when trapped molecules were released and flowed past the detector. (B) The height of the spikes in (A) plotted against applied frequency. Results from a single experiment are shown. The typical scatter in the fluorescent signal among repeated experiments is roughly 20% as shown in Fig. 7. Assuming that the efficiency is proportional to the strength of the trap, the satisfactory fit to Eq. (1) indicates that the DNA polarization is dominated by a single relaxation time over the range of frequencies plotted.

3.2.1 Frequency dependence

As shown in Fig. 6, the amount of DNA trapped increased with decreasing frequency, confirming earlier observations that the trapping is stronger at lower frequencies [2]. The data shown in Fig. 6 is well-fit by a dispersion equation of the form

$$\text{peak height} = \frac{A}{(1 + 4\pi^2 f^2 r^2)} + B \quad (1)$$

with a relaxation time $r = 3.0 \pm 0.7$ ms, where f is the frequency in Hz. The fit implies that under these conditions, trapping was governed by a single relaxation process. Assuming that trapping efficiency is proportional to the strength of the induced dipole, this result is in concordance with low-frequency bulk measurements of DNA polarizability which are also well fit with a first-order dispersion relation.

The frequency dependence was further investigated by making repeated measurements using four samples with DNA of different molecular weights. As shown in Fig. 7, trapping of all the samples became more efficient as the frequency was lowered from 2 kHz down to 10 Hz. Fitting these data with Eq. (1) provided an estimate of the relaxation time, r, for each sample. Despite large differences in DNA size, no significant difference in relaxation time was found (Fig. 7). Formally, the fit to the pBR322 (4.4 kb) DNA gives a somewhat longer relaxation time. Given the rather large variation in the low-frequency experiments, we consider this result to be suggestive but requiring confirmation. In addition, pBR322 DNA is also the the only circularized DNA used in our experiments.

3.2.2 Dependence on voltage and duration – the capacity of the traps

Figure 8A indicates that the quantity of DNA trapped increased linearly with trapping time to a 240 s application of a 3 V_{p-p}, 30 Hz signal. The lack of any observed saturation suggests that the capacity of the trap was not reached. The amount of DNA trapped was estimated by examining the data shown in Fig. 9. Photomultiplier gain was low enough during this measurement that background fluorescence did not contribute to the signal, and the measured level therefore represented DNA fluores-

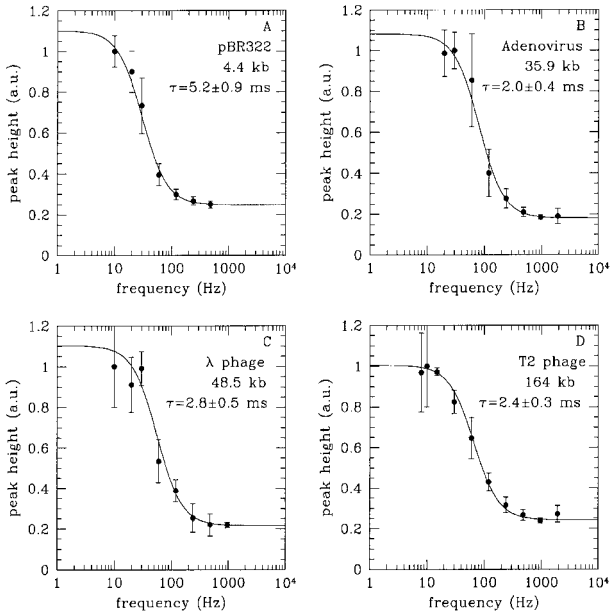

Figure 7. Frequency dependence of trapping efficiency at various molecular weights. Trapping efficiency for all samples increased as the frequency was lowered. A formal fit to the data gives a longer relaxation time for pBR322 (4.4 kb) than for the heavier strands, however, the large uncertainties at low frequencies make this conclusion tentative.

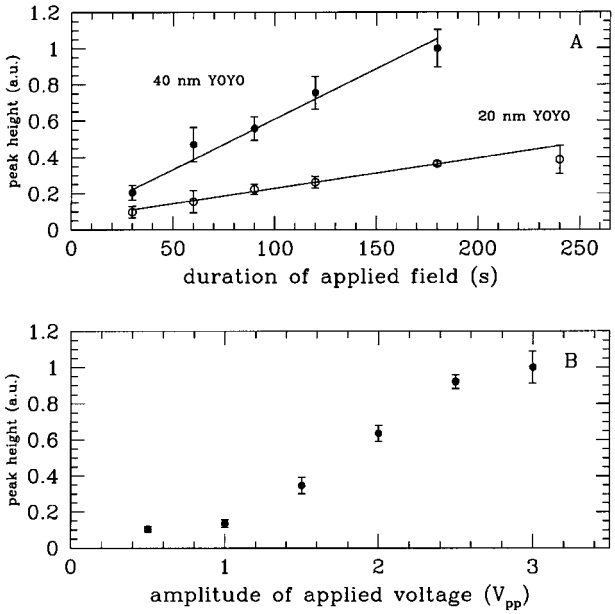

Figure 8. Trapping efficiency *vs.* duration and amplitude. (A) The amount of DNA trapped varied linearly with the duration of the applied field indicating that under these conditions, the capacity of the trap was not reached. (B) The quantity of DNA trapped with a 30 Hz signal increased significantly with increasing the amplitude below 2.5 V, although the data do not strongly support the quadratic dependence predicted by simple theory [1]. Significant dye fading occurred at higher voltages with bubble formation occurring above 5 V_{p-p}.

cence without any additional offsets. During the first 30 s, before the application of voltage, a signal level of 0.015 ± 0.004 (ave. ± SD) occurred due to DNA at 200 ng/mL flowing past the detector. After application of a 3 V_{p-p}, 30 Hz signal, the measured intensity decreased to 0.008 ± 0.002, indicating that ~ 50% of the DNA was being caught in the upstream trap. The release of trapped DNA after 240 s of applied field (data not shown) resulted in a peak 62× higher than the initial signal level, indicating that DNA had accumulated to a concentration of at least 12 μg/mL in the trap.

Similar experiments were performed to investigate the effects of varying the amplitude of the trapping signal. As shown in Fig. 8B, the amount of DNA trapped after 60 s at a frequency of 30 Hz increased as the voltage was raised from 0.5 to 2.5 V_{p-p}. At low voltages (< 2.5 V_{p-p}), the trapping efficiency increaded rapidly with applied voltage and although the data are consistent with a quadratic dependence, we cannot rule out a more complicated relationship. As the voltage was increased further, fading of the dye, and eventually bubble formation occurred at the electrode edges (> 5 V_{p-p}) complicating interpretation.

The strength of the electric field gradient experienced by the DNA near the electrode edges is difficult to estimate because it is strongly dependent on the sharpness of the electrode edges and the distance of closest approach of the molecules. A simple estimate based on a finite-element model of the electrodes suggests field gradients at a distance of ~ 1 μm of ~ 25 kV/m for a 1 V_{p-p} applied voltage. This crude estimate does not include potentially significant details such as transport of ions in solution or the effect of any chemical reactions which might occur at the electrodes even at voltages < 5 V_{p-p} at which point bubble formation was easily observed.

4 Discussion

The polarization of a dielectric sphere suspended in a conducting, dielectric medium was first presented by Wagner [17] who showed that the induced electric dipole of a particle depends on the permittivity and conductivity mismatch between the particle and its surroundings. The frequency response of the induced dipole, depends of the speed with which charge carriers can rearrange themselves in response to an external electric field and is usually characterized by the relaxation time, τ. Although Maxwell-Wagner theory predicts very weak low fre-

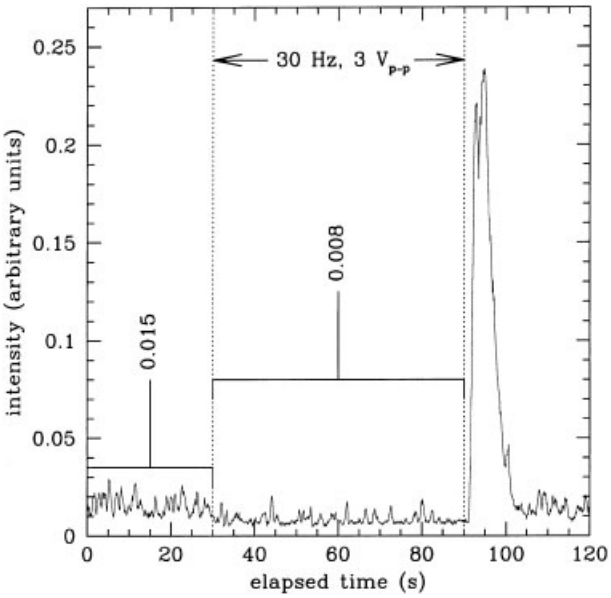

Figure 9. Estimation of the capacity of a DEP DNA trap in a flow experiment. During the application of a 30 Hz, 3 V_{p-p} signal, the measured intensity dropped to half its original level indicating that ~50% of the DNA was extracted from the flow. When released, the height of the resulting peak indicates a 16-fold increase in DNA concentration. Concentration increases as high as 62-fold were achieved for trapping durations of 240 s (data not shown).

quency polarizability for particles in aqueous solutions, typical biological particles, including DNA, exhibit strong, positive dielectrophoresis below 10 kHz [18–22].

Charged particles in solution attracts clouds of counterions which have some mobility along the particle's surface. Although these charge carriers are ignored in Maxwell-Wagner theory, there have been numerous theoretical and experimental efforts to understand their effect on the polarizability of model systems such as suspensions of polystyrene beads [23–26]. Two experimental observations support the idea that distortion of these counterion clouds dominates the low-frequency dielectric properties of biological particles in solution. First, the measured dielectric relaxation times roughly agree with the estimated diffusion times for small ions along the surface of larger charged particles. In addition, the degree of polarization, and thus the induced dipole moment is strongly affected by the concentration of counterions in solution.

Very little quantitative work has been done on dielectrophoresis of macromolecules such as DNA. Like other charged particles in solution, DNA possesses a counterion cloud which is presumably responsible for the large dielectric constant measured at low frequency in bulk solutions [6–14]. Modeling the dielectric properties of DNA is complicated by the fact that the molecule may distort under an applied electric field, and the mobility of the counterion cloud along the backbone is not well understood [27]. Despite these complications, we have chosen to test our data against the hypothesis that the polarizability of DNA and hence its dielectropheretic behavior can be characterized by a single relaxation time.

A significant challenge facing the application of DEP to typical biochemical processes involving DNA is its reliance on relatively low ionic strength. Despite this limitation, it is likely that schemes can be developed in which DEP is used to move DNA to sites in a microdevice where chemical modifications occur once the molecules are released and the solvent exchanged. Further study of the effect of ionic strength on the efficiency of dipole trapping will be essential to such developments.

At the frequencies and field strengths presented in this paper, the dipole trapping of DNA is reversible and appears to be fairly gentle, although these experiments would not have detected moderate amounts of strand breakage. Washizu *et al.* [28] have presented results on DEP at much higher frequencies (~ 1 MHz) and field strengths (~ 1 V/μm) and found that DNA became irreversibly attached to aluminum electrodes. Further work is needed to show that low-frequency DEP trapping does not induce significant damage in the DNA.

Field-induced aggregation of DNA over the electrode edges (for example, [29]) might enhance trapping efficiency through dipole-dipole interactions although we have successfully trapped individual molecules in very dilute solutions indicating that such interactions are not required for trapping. Additional experiments on the concentration depence of trapping and the capacity of the electrode traps would address the degree to which dipole-dipole interactions are important.

Manipulation of small quantities of DNA by electrical forces in microdevices is likely to be a technique of growing importance in molecular biology. The small electrode geometries in such devices almost unavoidably generate strong, highly divergent fields and thus inevitably subject DNA to induced dipole forces. Just as the advent of microfluidics forced designers to consider the ways in which fluids behave when surface tension becomes a dominant effect, the use of microelectrodes will require careful consideration of induced dipole forces.

This work was supported in part by a National Institutes of Health National Research Service Award training fellowship (T32 HG 00035) and grants from the US Department of Energy (DE-FG06-93ER61662) and the Washington Technology Center (95-B9).

Received November 16, 2001

5 References

[1] Pohl, H.-A., *Dielectrophoresis: The Behavior of Neutral Matter in Nonuniform Electric Fields,* Cambridge University Press, Cambridge, UK 1978.

[2] Asbury, C. L., van den Engh, G., *Biophys. J.* 1998, *74*, 1024–1030.

[3] Washizu, M., Kurosawa, O., *IEEE Trans. Ind. Appl.* 1990, *26*, 1165–1172.

[4] Washizu, M., Suzuki, S., Kurosawa, O., Nishizaka, T., Shinohara, T., *IEEE Trans. Ind. Appl.* 1994, *30*, 835–843.

[5] Rayner, S., Miller, G. A., Gordon, S. L., Ward, T., Evans, G. A., Heller, M. M., Garner, H. R., *Third International Conference on Automation in Mapping and DNA Sequencing,* LBNL, November 1995.

[6] Takashima, S., *J. Mol. Biol.* 1963, *7*, 455–467.

[7] Takashima, S., *J. Phys, Chem.* 1966, *70*, 1372–1380.

[8] Takashima, S., *Biopolymers* 1967, *5*, 899–913.

[9] Molinari, R. J., Cole, R. H., Gibbs, J. H., *Biopolymers* 1981, *20*, 977–990.

[10] Sakamoto, M., Kanda, H., Hayakawa, R., Wada, Y., *Biopolymers* 1976, *15*, 879–892.

[11] Sakamoto, M., Hayakawa, R., Wada, Y., *Biopolymers* 1978, *17*, 1507–1512.

[12] Sakamoto, M., Hayakawa, R., Wada, Y., *Biopolymers* 1979, *18*, 2769–2782.

[13] Tung, M. S., Molinari, R. J., Cole, R. H., Gibbs, J. H., *Biopolymers* 1977, *16*, 2653–2669.

[14] Vreugdenhil, T., van der Touw, F., Mandel, M., *Biophys. Chem.* 1979, *10*, 67–80.

[15] Gruenwedel, D. W., Hsu, C. H., Lu, D. S., *Biopolymers* 1971, *10*, 47–68.

[16] Takashima, S., *Biopolymers* 1966, *4*, 663–676.

[17] Wagner, K. W., *Arch. Elektrotech.* 1914, *3*, 83.

[18] Burt, J. P. H., Al-Ameen, T. A. K., Pethig, R., *J. Phys. E* 1989, *22*, 952–957.

[19] Burt, J. P. H., Pethig, R., Gascoyne, P. R. C., Becker, F. F., *Biochem. Biophys. Acta* 1990, *1034*, 93–101.

[20] Markx, G. H., Talary, M. S., Pethig, R., *J. Biotechnol.* 1994, *32*, 29–37.

[21] Pething, R., *4th Toyota Conference,* Aichi, Japan, 21–24 October 1990.

[22] Ting, I. P., Jolley, K., Beasley, C. A., Pohl, H. A., *Biochim. Biophys. Acta* 1971, *234*, 324–329.

[23] Fixman, M., *J. Chem. Phys.* 1980, *72*, 5177–5186.

[24] Lim, K. H., Franses, E. I., *J. Colloid Interface Sci.* 1986, *110*, 201–213.

[25] O'Konski, C. T., *J. Phys. Chem.* 1959, *64*, 605–619.

[26] Schwartz, G., *J. Phys. Chem.* 1962, *66*, 2636–2642.

[27] Mandel, M., Odijk, T., *Rev. Phys. Chem.* 1984, *35*, 75–107.

[28] Washizu, M., Kurosawa, O., Arai, I., Suzuki, S., Shimamoto, N., *IEEE Trans. Ind. Appl.* 1994, *31*, 447–456.

[29] Mitnik, L., Heller, C., Prost, J., Vivoy, J.L., *Science* 1995, *267*, 219–222.